JOURNAL OF MATERIALS SCIENCE **34** (1999) 3437–3445

An investigation on the laser surface alloying of copper on iron

K. K. PRASHANTH, K. CHATTOPADHYAY
Department of Metallurgy, Indian Institute of Science, Bangalore 560 012, INDIA

J. MAJUMDER
Mechanical and Applied Mechanics, University of Michigan, Ann Arbour, MI 48109-2125, USA
E-mail: kamanio@metalrg.iisc.ernet.in

Laser surface alloying of iron substrate with copper under different processing conditions has been systematically studied. The microstructural analysis reveals a predominantly cellular microstructure with copper wetting the cell boundaries. Globular distribution of copper at higher laser scanning speeds can be observed occasionally indicating the system under these conditions to be near the metastable miscibility gap. The concentration of copper in the pool is related to the laser scanning speed. In all cases a banded morphology indicating unsteady growth towards the bottom of the alloyed zone is observed. The hardness of the alloyed zone is significantly higher and is attributed to work hardening due to differential thermal contraction of the two phases in the alloyed zone. © *1999 Kluwer Academic Publishers*

1. Introduction

In many applications involving steel, there is a demand for enhancing the thermal conductivity of the surface. Surface alloying with copper provides one of the options for achieving this goal. With this in mind, we have carried out a detailed study of the laser surface alloying of copper on a iron substrate with the particular emphasis on the microstructure development and its relation to the processing parameters. The iron-copper system forms an immiscible system. The stable and metastable phase diagrams are well established [1–3] and the metastable phase diagram is given in Fig. 1.

2. Experimental

The surface alloying with copper on iron substrate was carried out using a 6 kW CO_2 laser (TRUMF make). The composition of the substrate is given in Table I. The purity of copper powder was 99.98%. Alloying was done with a power of 2 kW and a constant powder feed rate of 0.1 g/s. Different scan rates ranging from 5 to 38 mm/s were used. Experiments were carried out with both single pass and multiple passes with overlapping edges. The alloyed tracks were characterized using X-ray diffraction, optical, scanning and transmission electron microscopy.

3. Results

3.1. X-ray diffraction

The X-ray diffraction (XRD) study was carried out on the laser clad samples. Fig. 2 shows the XRD patterns for samples processed at different laser speeds, i.e. 13, 25 and 38 mm/s laser scan speeds respectively. These show the presence of Cu and α-Fe peaks along with the Fe_3O_4 oxide peaks. From the relative heights of the peaks in the XRD patterns it is clear that the copper content decreases as the laser scan speed increases. This was further verified by EDAX results. The presence of Fe_3O_4 peaks, which are due to the oxidation, follows the same trend.

3.2. Microstructure

Fig. 3 shows a collage of optical micrographs showing the microstructure of the clad pool of the sample processed at a laser speed of 9 mm/s. Few features can be worth noticing. The melted section is near hemispherical. The maximum depth of the pool is $\sim$1200 μm. One could see a banded feature in the solidified pool located at the bottom of the pool near the substrate. The microstructure is essentially cellular with cells becoming dendritic towards the topside in the middle of the pool. Fig. 4a and b shows the scanning electron micrographs at depth of 300 and 1000 μm from the top. The cellular structure can be clearly seen. The intercellular phase is continuous and covers the entire cell boundaries. In Fig. 4b the nature of the banding can be seen. The micrograph reveals that near the band boundaries the cell is discontinuous indicating a discontinuity in the growth process. New cells start growing in the next band. The inset shows a magnified micrograph of the region between the two bands. Fine droplets can be seen in these regions. Both the micrographs exhibit a tendency of dendritic instability. Fig. 4c shows a well

TABLE I Table showing the composition of the substrate as determined from the chemical analysis

Constituent	C	Si	Mn	S	P	Cr	Ni	Mo	Fe
wt %	0.024	0.004	0.048	0.012	0.006	0.001	0.003	0.001	Remainder

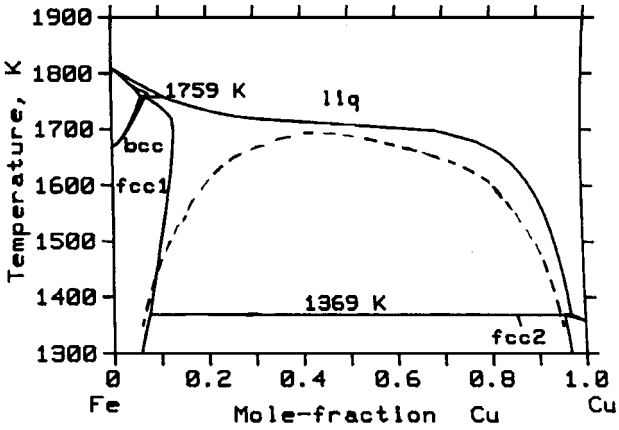

Figure 1 Stable and metastable phase diagram of iron-copper system (after reference 3).

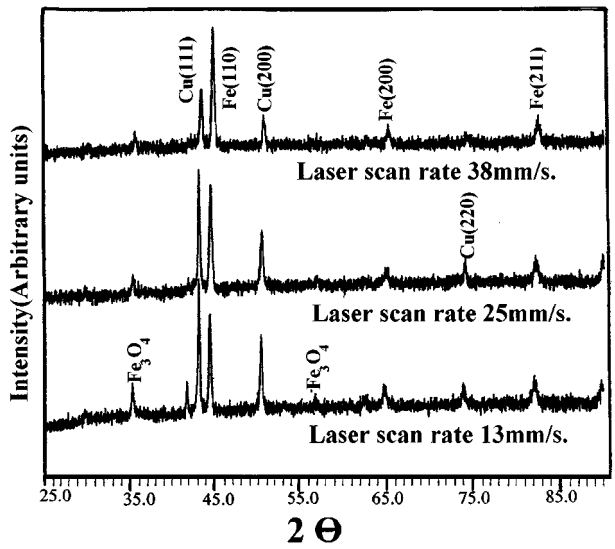

Figure 2 X-ray diffraction patterns obtained from the laser clad pools processed at laser scanning velocities of 13, 25 and 38 mm/s showing the presence of α-iron and copper peaks along with Fe_3O_4 peaks.

developed dendritic microstructure towards the top of the pool.

In contrast samples surface alloyed with a scan speed of 38 mm/s yield a much shallower pool (Fig. 5). The scale of microstructure is significantly finer. However, banded appearance towards the unmelted substrate can be seen even in this case. The scanning electron micrograph of Fig. 6a shows the details. The cells are considerably finer and elongated. However, like earlier case, the growth is disturbed at the band boundaries. A careful examination reveals that in certain regions one observe droplets of the minor phase both in the cell boundaries and in the cell interior (Fig. 6b). Such features are also observed, although rarely, in samples obtained with a slower scanning slightly away from the melt-substrate interface. The microstructure of the samples processed with scanning rates intermediate between these two extreme cases exhibit cellular microstructure with the refining of cell spacing with increasing scanning speed. The minor intercellular phase is continuous at the cell boundaries even at a scanning speed of 25 mm/s.

Fig. 7a–c gives the composition profiles from top to bottom along the center line for three samples processed at 9, 25 and 38 mm/s scanning speed. The composition is averaged over several cells. In the pool processed with 9 mm/s scanning speed, the composition is fairly uniform. For the scanning speed of 25 mm/s the average composition decreases to about 11%Cu. However, there is a distinct enrichment near the substrate. The composition drops dramatically at higher speed and for the scanning rate of 38 mm/s the average composition is 4%Cu. More significantly the composition is higher near the substrate and less at the middle of the pool.

Another interesting feature in the microstructure of these clad pools is the infiltration of cooper in-between the grain boundaries of the substrate i.e. iron. This can be very clearly seen in the SEM micrographs (Fig. 8a). Fig. 8b shows the variation of copper content along the line 1-2-3-4-5.

As noted earlier, the cell size is coarsest near the center and finest in the regions slightly away from the melt substrate interface. The cell in general grows normal to the melt-substrate interface. A typical profile of the cell spacing along the center line of the vertical cross section of a single track sample processed at a scanning speed of 9 mm/s is shown in Fig. 9. There exist local variations in cell spacing. However, the trend indicates coarser spacing towards the middle. The hardness profiles along the depth for the same sample are presented in Fig. 10. The average hardness for the samples processed at 25 and 38 mm/s laser scan speeds vary in the range (300–400) and (250–300) VHN respectively.

4. Discussion

4.1. The evolution of the microstructure

The rapid solidification of Fe-Cu alloys is well documented in the literature. Although the phase diagram (Fig. 1) indicates complete miscibility in the liquid state and a very large gap in between the liquidus and the solidus, the undercooled liquid develops a metastable miscibility gap [2–4]. The undercooling required to access this miscibility gap is at least (25 K) at a composition of 43 at %Cu, which is the composition of the critical point. Thus depending on the undercooling, one expects either a cellular/dendritic microstructure or a microstructure consistent with the phase separation in the liquid state. It is shown that for iron rich alloys, the latter microstructure consists of a globular morphology of copper both at the boundaries as well as in the interior

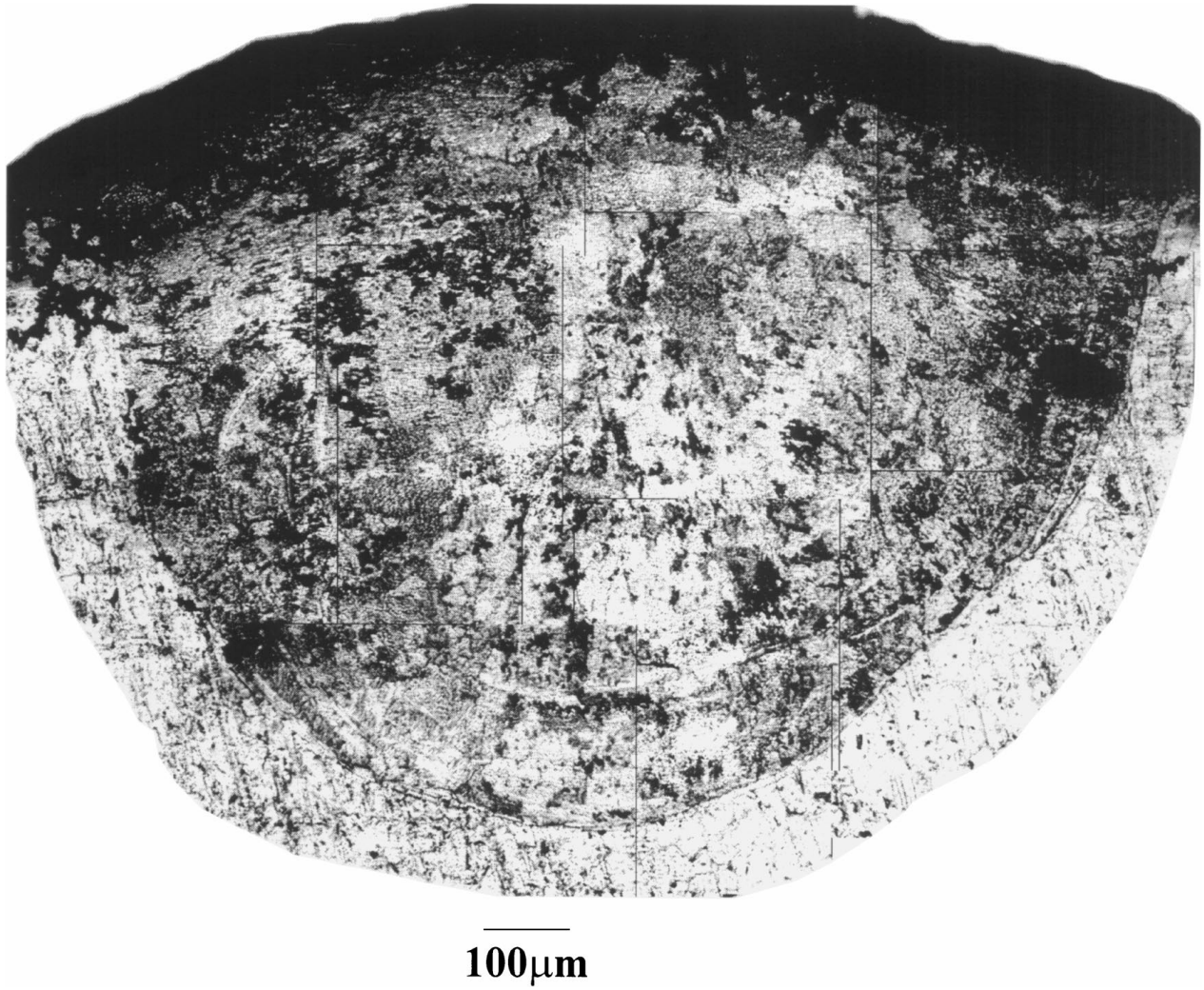

Figure 3 A collage of optical micrographs of the cross section of the clad pool of the laser treated sample processed at laser scan rate of 9 mm/s (single pass).

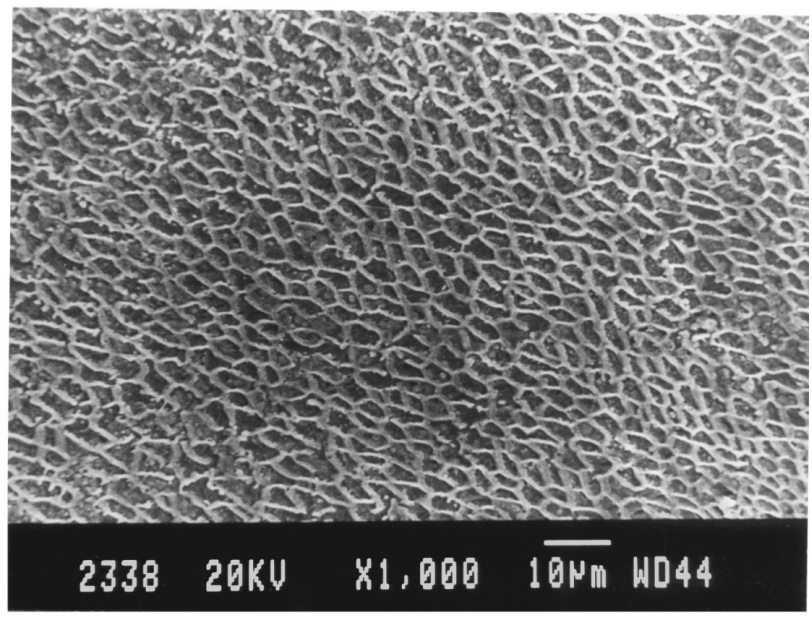

(a)

Figure 4 Scanning electron micrographs of the clad pool show: (a) Cellular microstructure at a depth of 300 μm from the top of the clad pool; (b) Banding observed at a depth of 1000 μm from the top of the pool. Inset shows the fine droplets observed in this region; and (c) Dendritic microstructure observed at the top of the clad pool. (Laser scan rate 9 mm/s, single pass). (*Continued*).

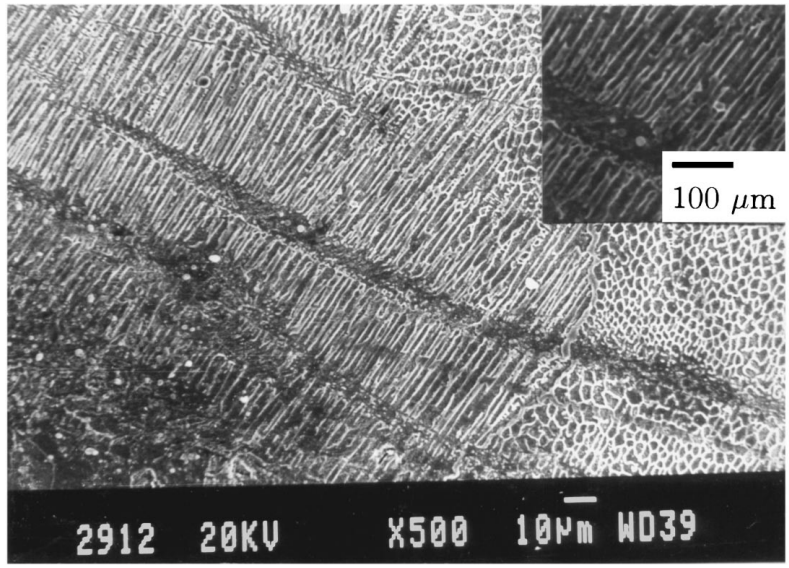

(b)

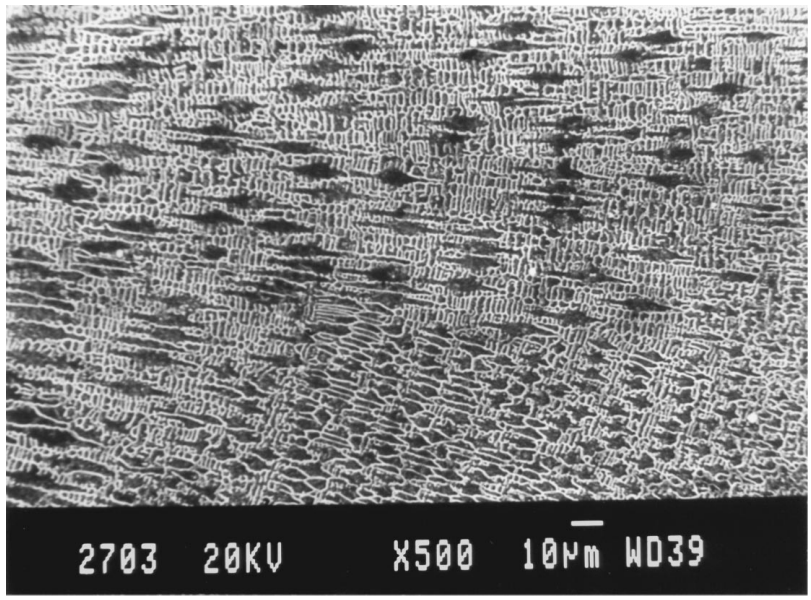

(c)

Figure 4 (*Continued*).

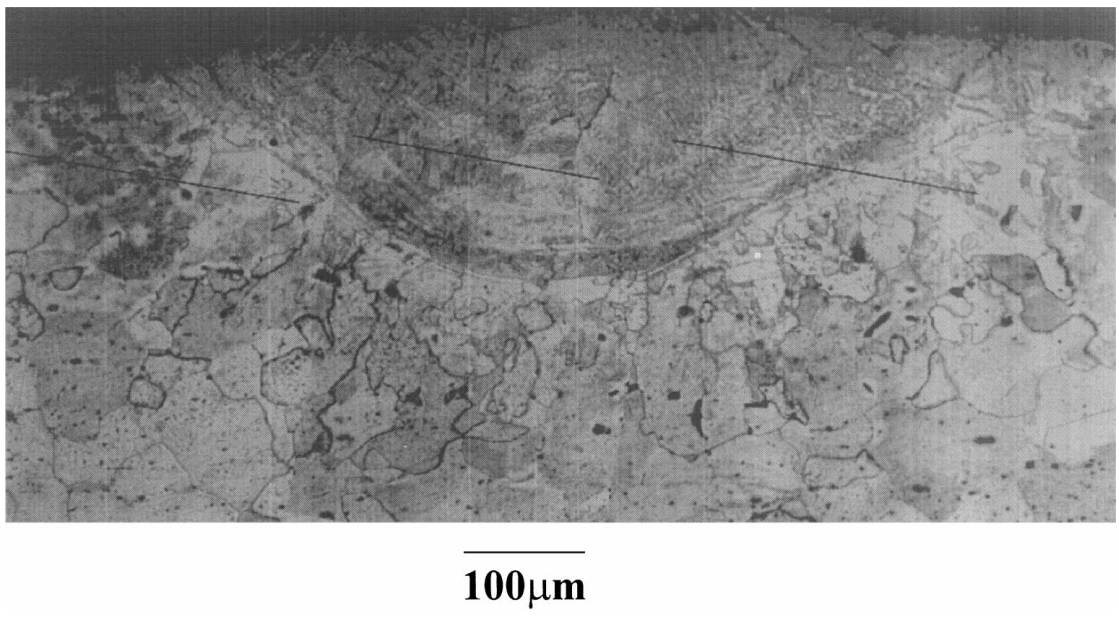

Figure 5 Optical micrograph of the clad pool processed at the laser scan velocity of 38 mm/s.

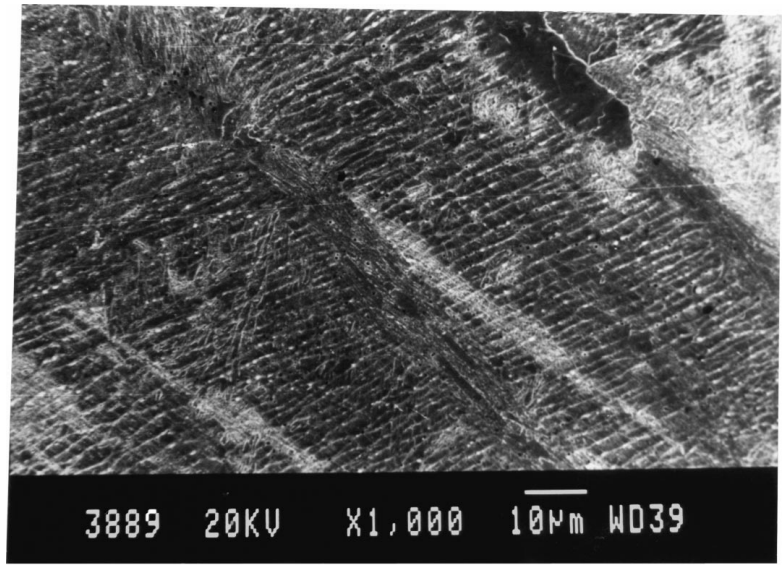

(a)

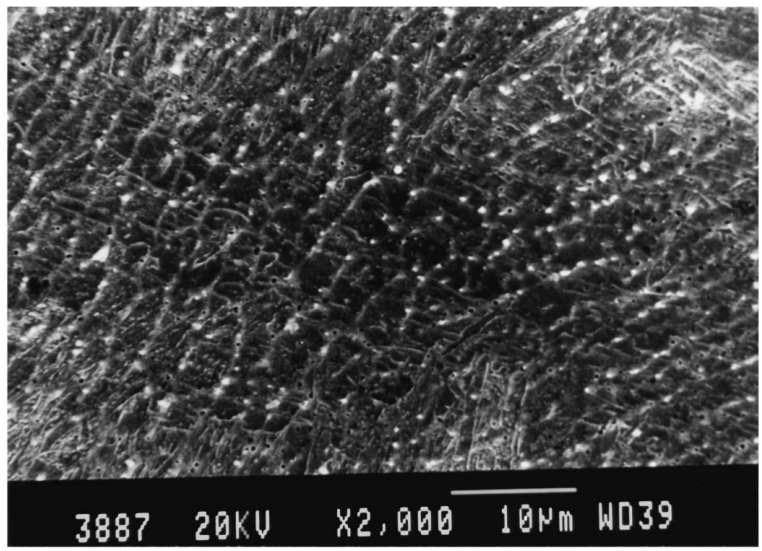

(b)

Figure 6 Scanning electron micrographs show: (a) fine and elongated microstructure in the clad pool, (b) fine droplets of the minor phase observed at the cell boundaries and cell interior indicating that the melt has been able to access the metastable miscibility gap region.

of the iron cells [4, 5]. Accessing the miscibility gap is easier for the copper enriched alloys.

The development of the microstructure during surface alloying, therefore, depends on two opposing factors. As the results of the composition analysis confirms, the higher scanning speed implies lesser copper enrichment in the alloyed layer. On the other hand, the slower scanning rate implies richer alloying. However, the higher scanning rates also represents higher heat transfer from the melt pool and higher rate of solidification. It is now well established that a difference in composition of the melt acts as a barrier to the epitaxial regrowth of the substrate [6]. Therefore, under high heat transfer condition melt gets undercooled. The initial growth of solid, as a consequence, takes place in the undercooled melt. This is clearly reflected both in the morphology and the spacing of the cells observed in the alloy pool. The cell spacings are finer in higher scanning rate samples indicating a higher growth rate due to growth in the undercooled melt. The feathery plate like appearance of the cells can be related to the change in the dendritic radius associated with the higher growth rate. Such a change has been theoretically established [7, 8]. The appearance of the droplets in these samples indicates the melt has entered the liquid miscibility gap. Since the pool contains only 4%Cu, this means attainment of very large undercooling. The lack of observation of this morphology in samples processed with slower scanning speed indicates that the undercooling of the melt is significantly less in these cases. Considering that the aim of the work is to enhance higher conductivity, the microstructure should be designed to have a continuous network of copper. In this regard the slower scanning speed yielding cellular microstructure with continuous intercellular copper is desirable.

The banded microstructure observed in the bottom portion of the pool clearly demonstrates the solid-liquid interface near the bottom of the sample does not move continuously. The microstructure suggests an

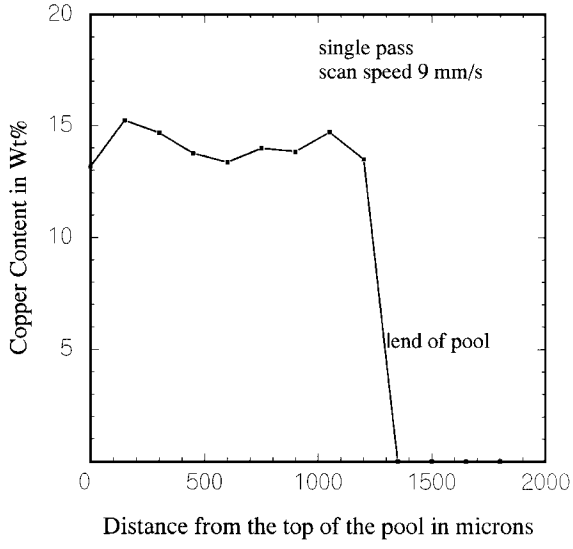

(a)

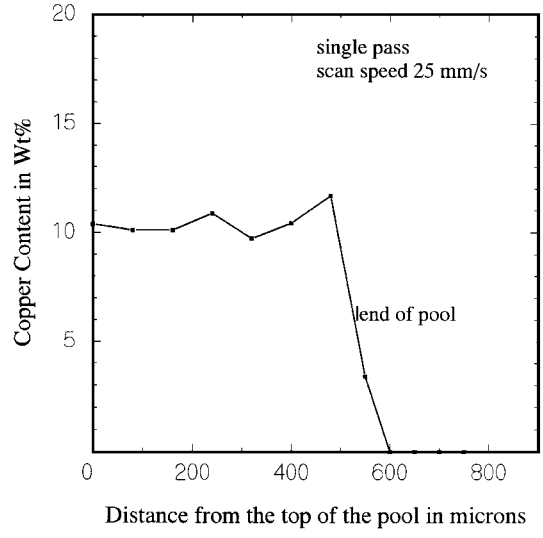

(b)

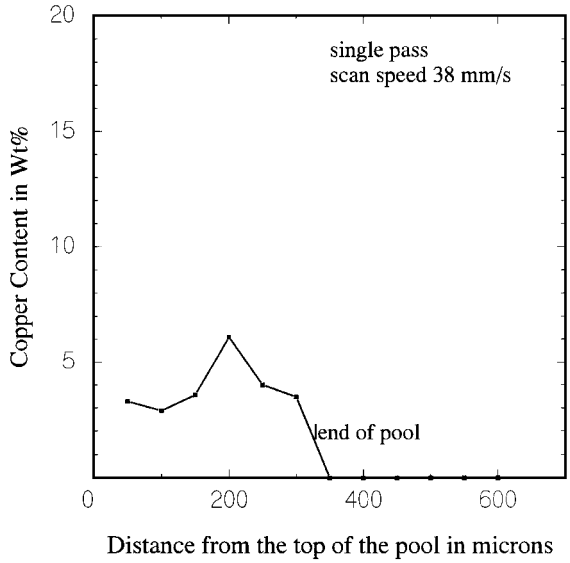

(c)

Figure 7 The variation of copper content along the depth of the clad pool processed at (a) 9 mm/s, (b) 25 mm/s and (c) 38 mm/s.

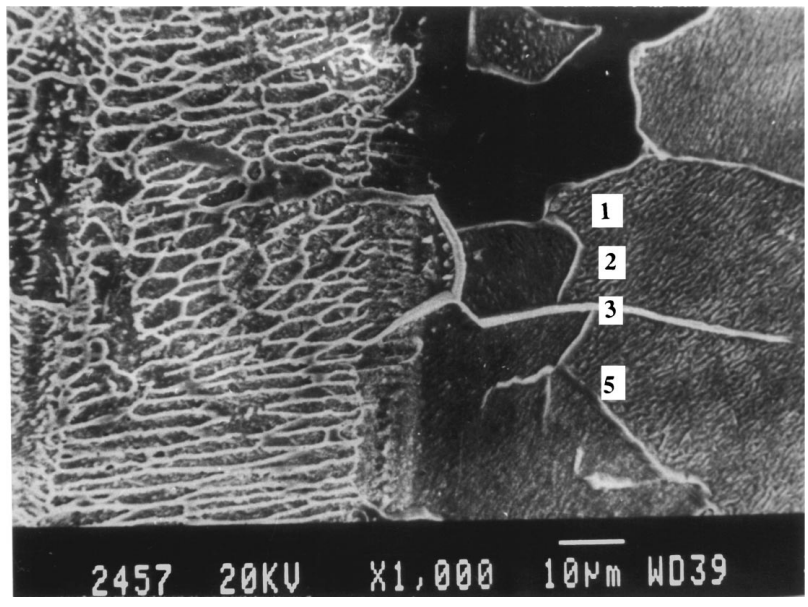

(a)

Figure 8 (a) Scanning electron micrograph shows the infiltration of copper between the grains of substrate iron. (b) The variation of copper content along 1-2-3-4-5 in 8a. (Please note that the probe size is larger than the boundary width. Therefore the composition at the boundary (no. 3) reflects the trend of copper enrichment and not the actual composition.) (*Continued*).

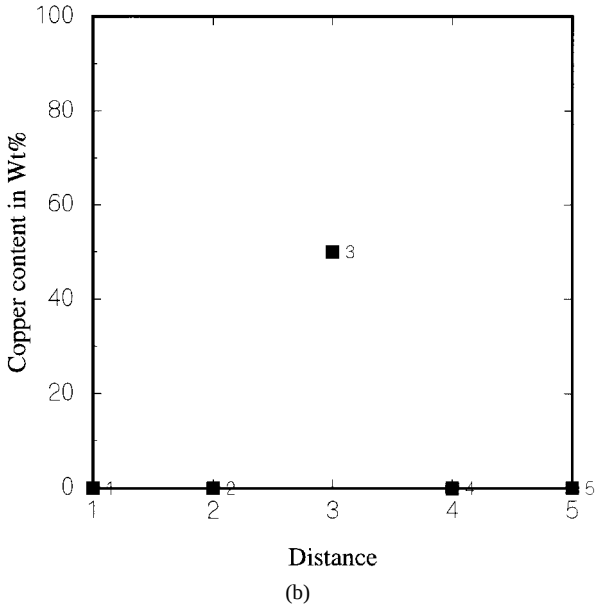

Figure 8 (*Continued*).

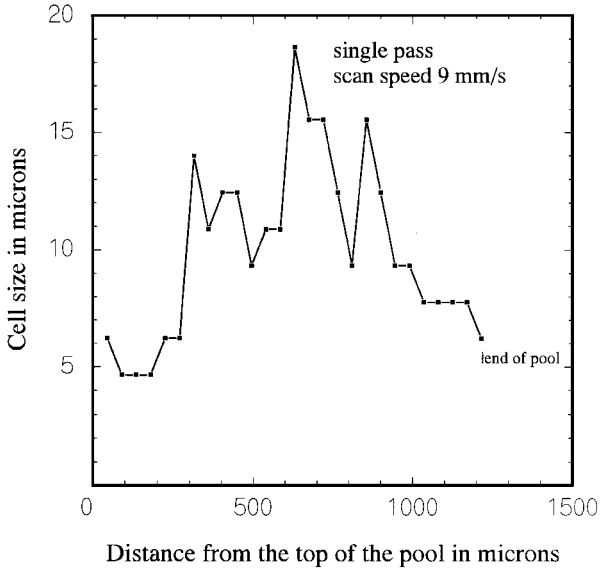

Figure 9 The variation of the cell size along the central line of the vertical cross section of the clad pool processed at 9 mm/s.

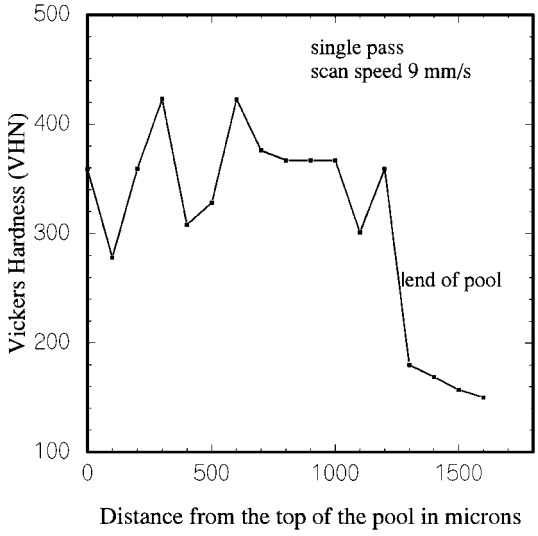

Figure 10 The variation of hardness along the depth of the clad pool processed at laser scan speed of 9 mm/s (single pass).

oscillatory motion of the interface. Recently a direct evidence of this type of behavior of the solid-liquid interface during laser processing has been obtained [9]. The convective transfer of the hot liquid from the top to the bottom of the pool is likely reason for such a change in growth behavior. A proper modeling of the evolution of this feature is not available in the literature.

The wetting of grain boundaries of a solid by a melt has been discussed by Smith [10]. Such wetting depends on the dihedral angle. For liquid copper on steel, the angle is very low ($\sim 20^\circ$). Thus one expects a penetration of copper melt to the grain boundaries of the substrate.

4.2. Composition of the alloyed layer

As mentioned in the preceding discussion, composition of the melt pool varied from 4%Cu to 14%Cu for scanning rate range of 38 m/s to 9 mm/s. The composition is fairly uniform for the slowest scanning speed. However, a distinct enrichment of the alloying element occurs in the bottom of the pool towards the substrate at higher scanning speed. Recent simulation work under the condition of surface alloying indicates such a trend [11]. This is attributed to the faster fluid flow from the top to bottom of the pool. In comparison solute rises relatively slowly yielding a solute enriched layer near the substrate.

4.3. Hardness of the surface alloyed layer

One of the major observations of the present work is the increase in hardness of the cladded region. The hardness of α-iron and Copper is 130 and 70 VHN respectively. Thus if one considers the rule of mixing, the hardness of the alloyed region should vary in between these two values. Clearly the hardness of all the samples are significantly higher and need rationalisation. In order to obtain better insight, we have carried out transmission electron microscopy of the α-iron grains in the clad region. Fig. 11a and b shows a bright field and dark field pair taken with $g = 110$. The selected area diffraction from the region at exact zone ($[001]_{Fe}$) is shown in Fig. 11c. The elongation of the spots can clearly be seen. The evidence suggested presence of significant amount of strain. These can arise from two sources (a) Thermal stress due to the difference in coefficient of expansions of the two phases. (b) Precipitation of copper in the α-iron matrix.

The precipitation of copper in iron matrix is well studied [12]. The results suggest a coherent precipitation of copper, which at the early stage may have 9R structure. Thus the iron BCC cells are expected to be strengthened by the coherent precipitates. However, since rapid solidification enhances the solubility, the strengthening effect due to this mechanism should be more prominent in the samples processed with higher laser scan speeds. This is not borne out from our observations. On the other hand, strain due to differential thermal contraction will depend on the volume fraction of the two phases. The strength is expected to be higher at lower scanning velocity which resulted in high volume of fcc copper in the microstructure. Thus we

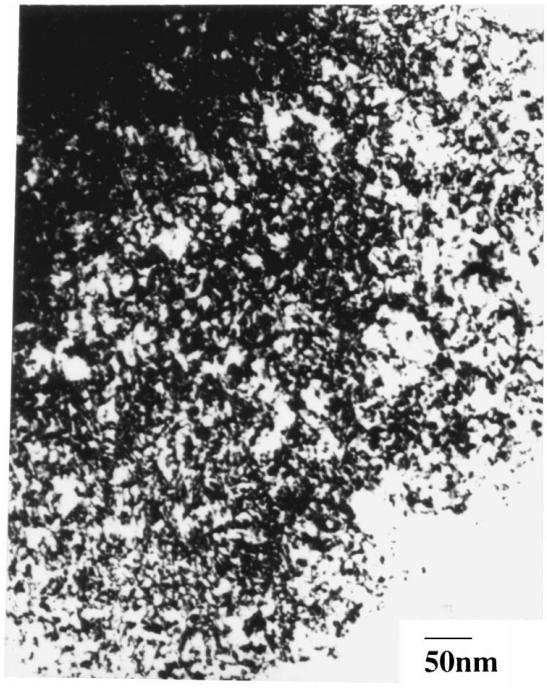

(a)

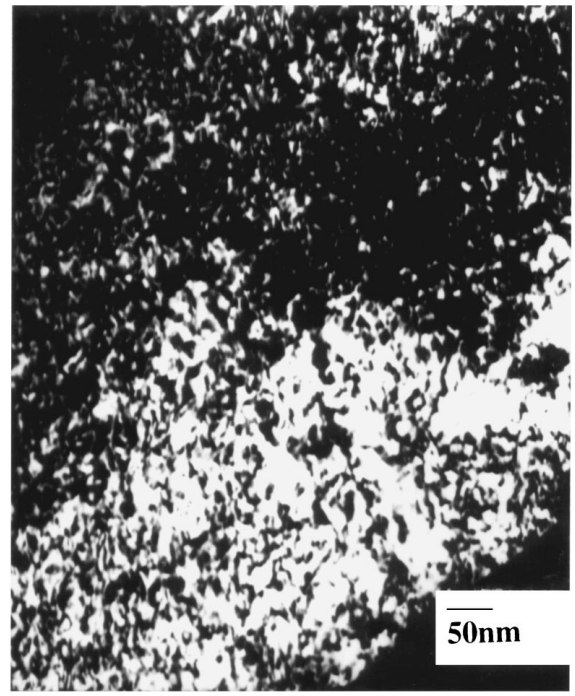

(b)

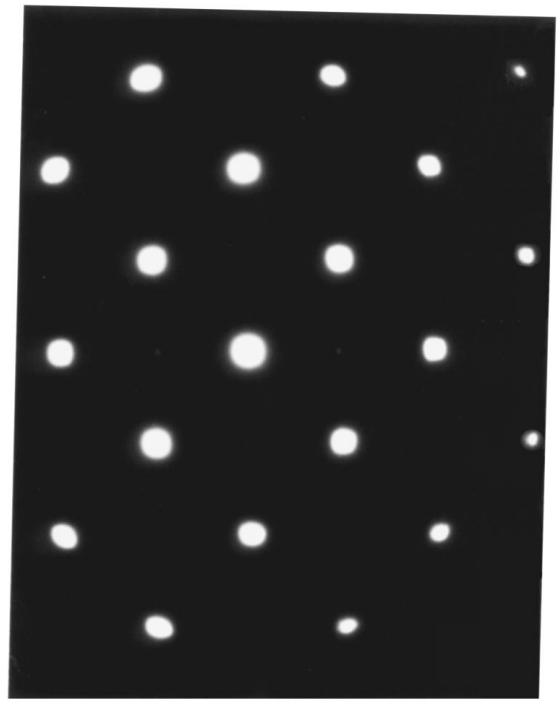

(c)

Figure 11 (a) Bright field. (b) Dark field TEM image of the α-iron grains in clad pool region with $g = 110$. (c) Selected area diffraction pattern of the region with $[001]_{Fe}$ zone. (Processed at laser scan rate of 5 mm/s, single pass).

conclude that the increase in hardness is primarily due to the thermal stress induced in the alloyed zone.

5. Conclusions

1. Copper can be surface alloyed on α-iron by laser to produce a two phase microstructure.

2. The phase distribution and copper concentration at constant feed rate depends on the laser scanning velocity.

3. Lower scanning velocity leads to an increase in the copper content and formation of cellular microstructure.

4. At higher scanning velocities, there is evidence of large melt undercooling and accessing of the metastable miscibility gap of the liquid.

5. Evidence of a banded cellular morphology towards the bottom of the pool is presented. The results indicate a non steady-state growth.

6. The hardness of the alloyed region is significantly higher and the transmission electron microscopy shows evidence of highly strained matrix.

7. The most likely cause for this strain (and increase in hardness) is work hardening due to the thermal stress originated due to the difference in the expansion coefficients of α-iron and copper.

Acknowledgements

The work derived support from a grant from Office of Naval Research, USA, under the Indo-US programme of research co-operation (Grant No. Nooo 14-95-1-0073). We also thank Mr. Sandip Bysakh for his help in transmission electron microscopy and Mr. G. Phanikumar for discussion.

References

1. T. B. MASSALSKI, "Binary Alloys Phase Diagrams" (ASM, Metals park, Ohio, USA) p. 983.
2. J. P. HAJRA and B. MAJUMDER, *Metall. Trans. B* **22B** (1991) 593.
3. Q. CHEN and Z. JIN, *Metall. Trans. A* **26** (1995) 417.
4. A. MUNITZ, *Metall. Trans.* **18B** (1987) 585.
5. Y. NAKAGAWA, *Acta Metall.* **6** (1958) 704.
6. C. G. WOYCHIK, D. H. LOWNDES and T. B. MASSALSKI, *ibid.* **33** (1985) 1861.
7. J. LIPTON, W. KURZ and R. TRIVEDI, *ibid.* **35** (1987) 957.
8. *Idem., ibid.* **35** (1987) 965.
9. P. S. MOHANTY and J. MAJUMDER, unpublished research.
10. C. S. SMITH, Metals Technology, Technical Publication No. 2387, Class E, 1948.
11. X. HE, B. L. MORDIKE, N. PIRCH and E. W. KREUTZ, *Lasers in Engineering* **4** (1995) 291.
12. P. J. OTHEN, M. L. JENKINS, G. D. W. SMITH and W. J. PHYTHIAN, *Phil. Mag. Lett.* **64** (1991) 383.

Received 17 June 1998
and accepted 27 January 1999